ISA Transactions 139 (2023) 510–523

Contents lists available at ScienceDirect

ISA Transactions

journal homepage: www.elsevier.com/locate/isatrans

Practice article

An event-based adaptation of the relay feedback experiment for frequency response identification of stable processes

L. de la Torre [a], J. Chacón [b,*], J. Sánchez-Moreno [a], S. Dormido [a]

[a] Department of Informática y Automática, Universidad Nacional de Educación a Distancia (UNED), C/ Juan del Rosal 16, 28040 Madrid, Spain
[b] Department of Arquitectura de Computadores y Automática, Universidad Complutense de Madrid (UCM), Plaza de las Ciencias 1, 28040 Madrid, Spain

ARTICLE INFO

Article history:
Received 30 May 2022
Received in revised form 8 March 2023
Accepted 7 April 2023
Available online 13 April 2023

Keywords:
Frequency response
Relay feedback
Identification
Event-based sampling

ABSTRACT

An event-based modification of the classical relay feedback experiment without the inclusion of additional elements (integrator, time delay, …) for identification of the spectrum of stable processes between zero and the phase cross-over frequency is presented. By inserting an event-based sampler in the control loop, the natural behaviour of a classical relay is simulated and the system is forced to work in two modes. The event-based sampler activates the first mode by sending control actions to the process every time the error signal crosses zero; this mode is to discover the approximated value of the cross-over frequency ω_{180°. During the second mode, the event-based sampler sends samples to the process simulating that the error signal crosses zero at ω_{180°/N where N is the number of points to identify in the range $0 \leq \omega \leq \omega_{180^\circ}$. One advantage of this procedure is that the logic used in an already existing relay feedback experiment to fit a transfer function model or tune a controller could be maintained just replacing the relay block by the event-based sampler block presented in the paper. Simulations and experiments with different processes and in presence of noise demonstrate the effectivity of the procedure.

1. Introduction

The relay feedback experiment is a very well-known method in system identification. In its basic mode it allows to approximate the phase cross-over frequency ω_{180° and the critical gain K_{180° of a process $G(s)$ from the describing function (DF) analysis [1]. Many modifications and extensions of this procedure have been developed during last 30 years with different purposes [2,3]. But the works of interest for the subject of this paper is the research focused in extracting two or more points located at frequencies lower than the oscillation frequency, ω_{osc}, determined by a relay-feedback procedure.

The most common procedures to identify additional points in the Nyquist map at lower frequencies than ω_{osc} are the inclusion in the loop of an additional time delay [4–7] or an integrator [8–11]. In both cases, the rationale is to force a clockwise rolling of $G(s)$ around the zero of the Nyquist map by adding a phase shift which produces a new virtual plant $G'(s)$ whose intersection with the negative reciprocal of the relay describing function occurs at a lower frequency ω'_{osc} than the original ω_{osc}. In the case of the delay, $G'(s) = G(s)e^{-sL_{\text{add}}}$ introduces an additional phase delay of $L_{add}\omega'_{osc}$, where ω'_{osc} is the new oscillation frequency. Here, the point $G(j\omega'_{osc})$ is located at a lower frequency than the frequency ω_{osc} obtained during the normal relay experiment without delay; that is, $\omega'_{osc} < \omega_{osc}$. In the case of the integrator, the additional phase delay is always $\pi/2$. Regardless the procedure chosen and once the relay test is concluded, the point $G'(\omega'_{osc})$ can be estimated in both cases as

$$\hat{G}'(j\omega'_{osc}) = \frac{Y(j\omega'_{osc})}{U(j\omega'_{osc})} = \frac{\int_0^{2\pi/\omega'_{osc}} y(t)e^{-j\omega'_{osc}t}dt}{\int_0^{2\pi/\omega'_{osc}} u(t)e^{-j\omega'_{osc}t}dt} \tag{1}$$

where ω'_{osc}, $y(t)$, and $u(t)$ are data obtained from the test [12]. It must be noticed that Eq. (1) cannot be applied to determine the steady gain $G'(0)$, unless a bias is added to the relay. If there is no bias, the oscillations produced by the relay are symmetric, and the integration of the periods at $\omega'_{osc} = 0$ and the even harmonics will all be zero [13,14]. Finally, to estimate $G(j\omega'_{osc})$ the effect of the added phase delay must be discounted, that is,

$$\hat{G}(j\omega'_{osc}) = \frac{\hat{G}'(j\omega'_{osc})}{e^{-j\omega'_{osc}L_{add}}} \tag{2}$$

or

$$\hat{G}(j\omega'_{osc}) = \frac{\hat{G}'(j\omega'_{osc})}{j\omega'_{osc}} \tag{3}$$

* Corresponding author.
E-mail addresses: ldelatorre@dia.uned.es (L. de la Torre), jeschaco@ucm.es (J. Chacón), jsanchez@dia.uned.es (J. Sánchez-Moreno), sdormido@dia.uned.es (S. Dormido).

https://doi.org/10.1016/j.isatra.2023.04.008

Notation

N	Number of points to identify in the experiment. Fixed by the user.
$G'(s)$	Virtual process created by adding an artificial delay to the process
$\hat{G}(j\omega_k)$	Estimated point of $\hat{G}(j\omega_k)$
K_{180°	Critical gain
L_{add}	Artificial delay
T_1	Period of the synthetic signal generated by the EBS
t_{last}	Last time that $u(t)$ was sent to $G(s)$
ω_1	Frequency of the synthetic signal generated by the EBS
ω_{180°	Cross-over frequency
ω_k	Frequency between ω_{osc} and ω_1 identified after the experiment with the EBS
ω_{osc}	Oscillation frequency of $G(s)$ produced by a simple relay experiment
$\pm D$	Control action values sent to $G(s)$ by the EBS
$e(t)$	Error signal
EBS	Event-based sampler
FOPTD	First order plus time delay
$G(0)$	Steady gain of $G(s)$
SOPTD	Second order plus time delay
$G'(0)$	Steady gain of $G'(s)$
$G(s)$	Process to identify
$u(t)$	Control action
$y(t)$	Process output
δ	Hysteresis band of a relay
ρ	Asymmetry factor which determines the length of the semi periods of $u(t)$
ω'_{osc}	Oscillation frequency of $G'(s)$ produced by a relay experiment
n_0	Noise level

Other approaches to discover additional points below the cross-over frequency focus on modifying the hysteresis or the vertical asymmetry of the relay [1], a parasitic relay [12], using a cascade relay [15], or adding filters [16,17].

It is also possible to obtain more than two points of the spectrum between the cross-over frequency and zero using a simple relay experiment [18–22]. In these methods, the process information comes from the transient relay response before reaching the stationary cycle. The signals $y(t)$ and $u(t)$ are decomposed into the periodic stationary cycle and the transient parts because they are neither periodic nor absolutely integrable. The procedure explained in this paper has the same goal: to identify N points of the frequency spectrum of a process from zero to the cross-over frequency.

This paper presents an event-based sampler approach where a classical relay feedback experiment is modified by replacing the relay by an event-based sampler (EBS) to identify a set of points in the spectrum of $G(s)$ going from 0 to the phase-crossover frequency ω_{180°. The purpose of this approach is to provide an event-based identification procedure that can be easily integrated into an existent event-based control structure, for example, one based in a SSOD-PI controller [23,24] providing a complete event-based autotuning solution.

The structure of the paper is as follow. Section 2 is dedicated to explaining the event-based sampling strategy while Section 3 discusses the selection of the parameter's setup. Section 4 presents the results of identification experiments with different processes and a comparison with other similar identification methods. In Section 5, a study of the impact of noise in the procedure performance is presented. Section 6 shows the results of the application of the method to a real system: a DC motor. A discussion of the procedure is included in Section 7. Finally, Section 8 presents the conclusions.

2. Frequency response data identification through event-based sampling

It is theoretically feasible from Eq. (1) to obtain a specific point of $G(s)$ located at any frequency of the spectrum (e.g., harmonics located into the fourth quadrant of the Nyquist map) just by forcing the system to oscillate at the desired frequency. As it was indicated in Section 1, it is not possible to reach very low frequencies just by analysing the periodic stationary cycle produced by the classical relay feedback experiment.

However, if the sampling is done by fulfilling some requirements of time, the feedback response can be forced to oscillate at a low frequency. A solution to achieve that is to replace the relay with an EBS that manages when control actions are sent to the process and, therefore, force the oscillation frequency (see Fig. 1). Thus, each event triggered will produce sending of a control action $u(t)$ to the process, forcing the oscillation of the system at a specific frequency. The advantage of such setup is that the original procedure used to identify the critical points by the relay feedback response experiment does not need to be modified and can be maintained.

The rationale of the method to identify the spectrum of a stable process between zero and ω_{180° is that the EBS must be designed to generate two types of patterns of events. Each type is designed to force switching at different frequencies: ω_{osc}, that corresponds to the generated by a simple relay experiment (i.e, the approximation of ω_{180°), and a lower frequency, ω_1, defined by the user (see Fig. 2).

To generate two patterns of events, the EBS must consecutively work in two modes:

Mode 1. In this mode, it is possible to approximate the cross-over frequency ω_{180° by simulating the behaviour of a classical relay. During this mode, a signal $u(t) = \pm D$ is sent to the process only when the following triggering rule is satisfied:

$$\textbf{if } sgn(e(t)) \neq sgn(e(t_{last})) \wedge e(t) \neq 0 \textbf{ then } u(t) = sgn(e(t)) \cdot D \quad (4)$$

where t_{last} is the last time that $u(t)$ was sent to the process. At the end of this working mode, it is possible to approximate ω_{180° by

$$\omega_{180^\circ} \cong \omega_{osc} = \frac{2\pi}{T_{osc}} = \frac{\pi}{t - t_{last}} \quad (5)$$

because the semi period length is defined by $t - t_{last}$.

Mode 2. This mode starts when the EBS working with Mode 1 has concluded and ω_{osc} has been determined. The goal of this mode is to force the process to oscillate at a frequency $\omega_1 \ll \omega_{osc}$. In this case, the triggering rule is

$$\textbf{if } (t - t_{last}) \geq \rho T_1 \textbf{ then } u(t) = -sgn(u(t_{last})) \cdot D \quad (6)$$

where ρ is an asymmetry factor which determines the length of each of the semi periods of $u(t)$, and T_1 is the period of the synthetic signal that the EBS generates when it remains in this mode. Every time the triggering rule is fulfilled, a control action is sent, and the asymmetry factor switches in this way:

$$\rho \leftarrow 1 - \rho \quad (7)$$

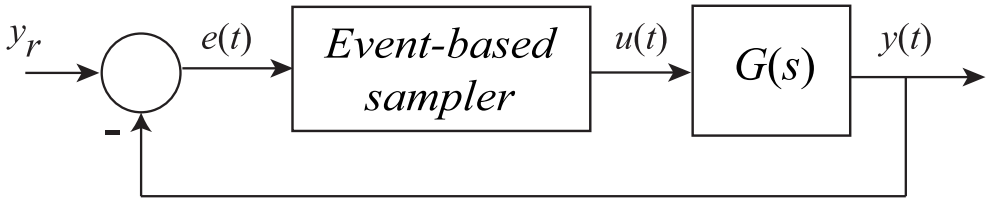

Fig. 1. Event-based feedback control loop.

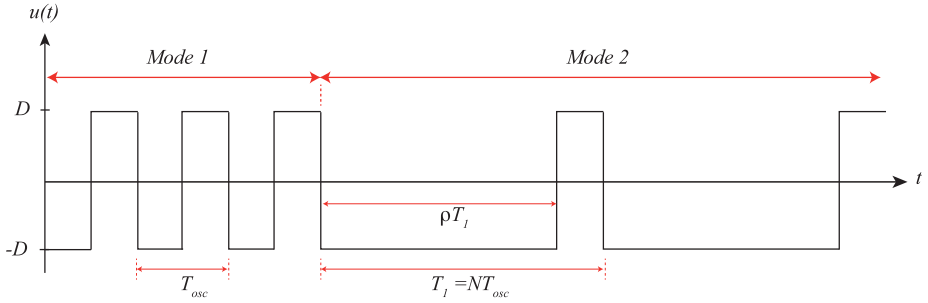

Fig. 2. Working modes generated by the event-based sampler.

The reason for introducing asymmetry is to identify $G(0)$ and points of $G(s)$ corresponding to even harmonics of ω_1. It is well known that a symmetric signal produced by a simple relay cannot be used to obtain such points as the sum of the semi periods is zero.

Once the experiment running in Mode 2 is concluded, it is possible to obtain a range of the spectrum of $G(s)$ from the experimental data by extending Eq. (1) in this way

$$\hat{G}(jk\omega_1) = \frac{\int_0^{2\pi/\omega_1} y(t)e^{-jk\omega_1 t}dt}{\int_0^{2\pi/\omega_1} u(t)e^{-jk\omega_1 t}dt} \tag{8}$$

with $k = 0, 1, 2..., N$ [25] or by the n-shifting procedure [7,26]. It must be noticed that the steady gain $\hat{G}(0)$ is obtained with $k = 0$ and $\hat{G}(jk\omega_{180^\circ})$ with $k = N$.

3. Parameter choices

3.1. Number of frequency response points

The number of frequency response points to identify in the spectrum of $G(s)$ must be initially specified to define T. Assuming N as the number of points to identify in the interval $[0, \omega_{osc}]$, the frequencies of the N points are defined by

$$\omega_k = k\frac{\omega_{osc}}{N} \tag{9}$$

with $K = 1, 2, \ldots, N$. As $w_1 = \omega_{osc}/N$, the period of the synthetic signal is given by

$$T_1 = \frac{2\pi N}{\omega_{osc}} \tag{10}$$

In this way, the synthetic signal generated by the EBS during Mode 2 would contain all the harmonics corresponding to the frequencies $(\omega_1, \omega_2, \ldots, \omega_{osc})$. The number of frequency response points, N, is a user-defined parameter. The direct consequence of the identification of more points is an increase of the duration of the experiment (see Section 3.3).

3.2. Selection of ρ

As ρ is expressed as a normalization of T_1 between 0 an 1 in Eq. (7), the conditions that must be satisfied to introduce assymetry in the semi periods are that $\rho \in (0, 1)$ and $\rho \neq 0.5$. According to [27], experimental results indicate that an asymmetry as high as possible should be chosen to get good low-frequency excitation and good estimates of $G(j\omega_{osc})$ and $G(0)$. However, it has been demonstrated in [28] that there exist several combinations of ρ and N that should be avoided to improve the accuracy on the estimation of each harmonic $G(j\omega_k)$. So, according with the results described in [28], the values of ρ to be avoided for a given number of points N can be expressed as

$$\rho \neq \frac{j}{i} \tag{11}$$

with $i = 1...N$ and $j = 0...i$. So, for example, if we consider $N = 3$, the list of ρ to avoid are: 0, 1/3, 1/2, 2/3, 1. However, if we consider $N = 4$, two more values (1/4 and 3/4) should be added to the list.

A study on the influence of ρ is presented in Example 4. The conclusions of the study agree with the results described in [23].

3.3. Duration of the experiment

The number of cycles to run the experiment depends on three factors: the time needed to converge to regular cycles, the presence of noise, and the number of points N. The first factor, the number of cycles needed to converge to a regular period, depends on the process. According to [27,29] it is enough to wait 2–3 cycles in most of the cases. In the examples, Modes 1 and 2 of the EBS are configured to run 2 and 3 cycles, respectively. The additional cycle added to the Mode 2 is due to the irregular transition between both modes, but the data corresponding to this extra cycle have not been considered for the calculations of Eq. (8).

The second factor, the presence of noise, can produce that more cycles must be considered to average in Eq. (8) the $y(t)$ samples collected from the oscillations exhibited in the tests. It is observed in [29] that if more samples are involved in the averaging, we can achieve a reduced relative error in the frequency response. In the tests executed in this paper, we have considered only cycles to reduce the experimentation time to the minimum.

Regarding N, in Eq. (10) we can appreciate that the number of identified points, N, has an impact on the duration of the cycles in Mode 2. A high N implies a high value of T_1 because the frequency

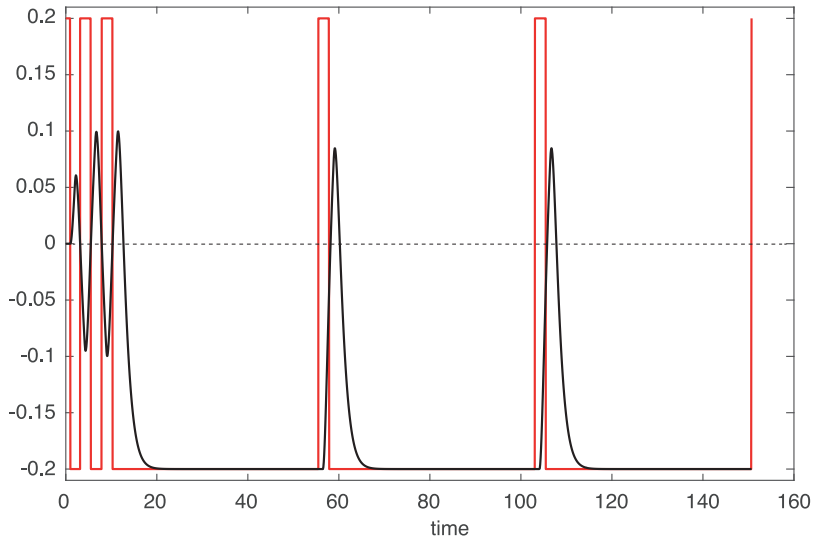

Fig. 3. Simulation of G_1 oscillating at $\omega_{osc} = 1.32$ during Mode 1 and at $w_1 = 0.132$ during Mode 2.

Table 1
Relative errors of the identification experiments for $N = 10$ with valid and invalid ρ's.

ρ	Err_N [%]			
	$G_1(s)$	$G_2(s)$	$G_3(s)$	$G_4(s)$
0.7 (7/10)	13.24	21.68	5.092	5.130
0.725	0.048	0.034	0.015	0.015
0.75 (6/8)	13.55	6281	10.16	11.54
0.777 (7/9)	6.279	7.698	7.362	3.359
0.8 (8/10)	16.55	106.4	9.962	12.09
0.833 (5/6)	5.430	10.76	9.133	7.025
0.85	0.054	0.033	0.016	0.017
0.857 (6/7)	11.75	62.22	6.928	9.685
0.875 (7/8)	4.760	29.28	5.845	5.259
0.888 (8/9)	5.198	6.309	8.699	2.775
0.9 (9/10)	6.639	9.801	4.699	5.857
0.925	0.039	0.032	0.012	0.013
0.95	0.045	0.041	0.014	0.016
0.99	0.172	0.158	0.051	0.048

ω_1 corresponding to the critical point $G(j\omega_1)$ will tend to zero ($\omega_1 = \omega_{osc}/N$). At the end of Example 1 (see Table 1) and in Section 7 (see Table 7), we present a comparative study of the influence of N in the total duration of an experiment.

4. Results from simulations

4.1. Example 1: Identification of a second order process plus time delay (SOPTD)

Consider the system

$$G_1(s) = \frac{e^{-s}}{(s+1)^2} \tag{12}$$

The setup of the experiment is fixed to $D = \pm 0.2$, $\rho = 0.95$, and $N = 10$. Modes 1 and 2 of the EBS are configured to run 2 cycles. During Mode 1, the EBS detects that $\omega_{osc} = 1.32$ and this allows programming the EBS for the Mode 2 obtaining a real $T_1 = 47.59$ s (Fig. 3). Applying Eq. (2) to the experimental data, we obtain $G_1(0)$ and the N points that can be shown in Fig. 4.

It must be noticed that the procedure can be used to fit common transfer function models used for tuning of PID controllers. For example, of the 11 identified points in the experiment, the 7th and 10th points that correspond to $\omega_{137.6^\circ} = 7\omega_1$ and $\omega_{180.03^\circ} = 10\omega_1$ are selected for fitting a FOPTD and a SOPTD models, respectively. These two points are chosen because the recommendation is to estimate the behaviour of the process at ω_{135° and ω_{180° depending on whether PI or PID control are to be applied. So, using the procedure described in [23], the fitted models are:

$$\hat{G}_{FOPTD(s)} = \frac{1.0000023e^{-1.538s}}{1.681s+1} \tag{13}$$

and

$$\hat{G}_{SOPTD(s)} = \frac{1.0000023e^{-1.0027s}}{(1.0002s+1)^2} \tag{14}$$

Fig. 5 shows the step responses of the original system and of the two models. The response of G_1 overlaps with the one of $\hat{G}_{SOPTD(s)}$.

4.2. Example 2: Identification of a non-minimum phase process

The second example corresponds to a non-minimum phase system

$$G_2(s) = \frac{1-s}{(s+1)^3} \tag{15}$$

The setup of the experiment is $D = \pm 1$, $\rho = 0.95$, and $N = 10$. At the end of Mode 1, the EBS measures $\omega_{osc} = 0.974$ that produces a real $T_1 = 64.45$ s in Mode 2. Figs. 6 and 7 present the temporal evolution of the experiments and the identified points, respectively. It must be noticed that the steady gains of G_1 and G_2 are equal, that is, $G_1(0) = G_2(0) = 1$, but the oscillation amplitudes in the simulations are different due to the control actions applied; that is consequence of the relay control values used in each experiment: $D = \pm 0.2$ for G_1 and $D = \pm 1$ for G_2. So, the control action applied to G_2 is five times the control action applied to G_1, producing the differences in the oscillation amplitudes.

4.3. Example 3: Comparison with other similar identification methods of the frequency spectrum

The study cases presented in this comparison are based in two processes used in [19,20], where frequency response identification methods based on a relay experiment are described. The first process to identify is

$$G_3(s) = \frac{e^{-5s}}{5s+1} \tag{16}$$

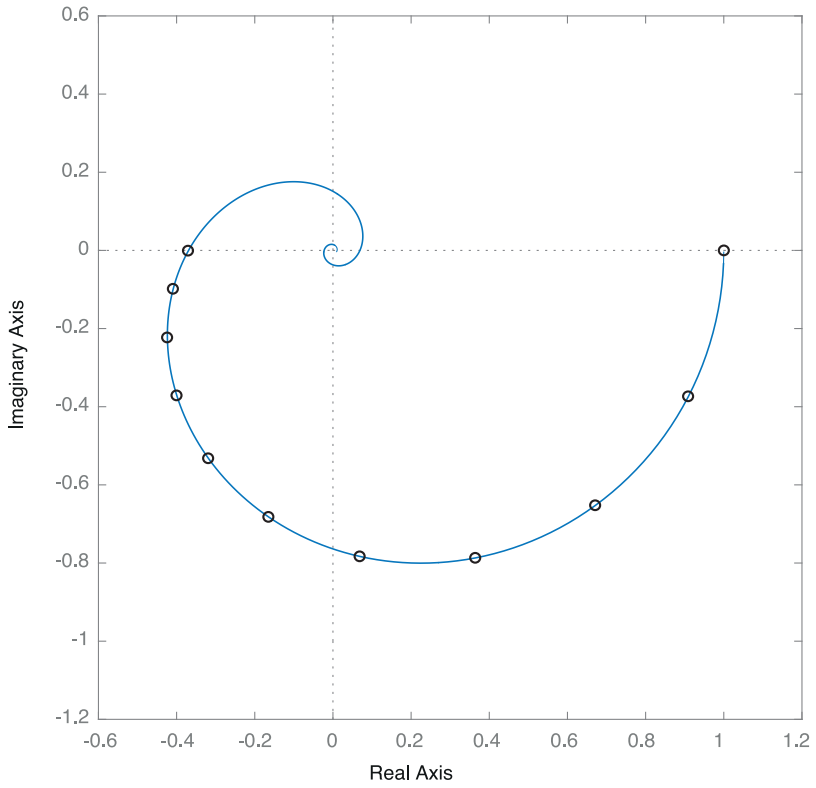

Fig. 4. Nyquist map showing G_1 and the 11 identified points.

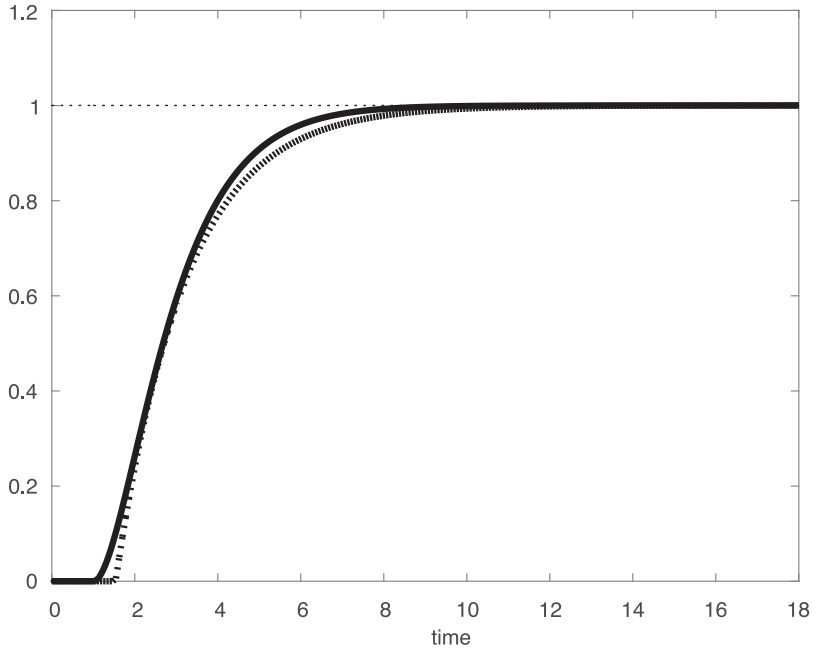

Fig. 5. Step responses of G_1 (red line), $\hat{G}_{FOPTD}$ (dotted line), and $\hat{G}_{SOPTD}$ (black line).

The setup of the experiment is $D = \pm 1$ and $N = 10$ that corresponds to the same setup employed in the research papers used for the comparison. The assymetry factor is $\rho = 0.95$ and Modes 1 and 2 are fixed to run 2 and 3 cycles as in previous examples. The EBS measures $\omega_{osc} = 0.421$ at the end of Mode 1, that produces a $T_1 = 149$ s in Mode 2. Figs. 8 and 9 show the evolution of the experiments and the identified points, respectively.

The second process to identify is a high-order system:

$$G_4(s) = \frac{1}{(s+1)^8} \tag{17}$$

and the setup applied is the same that for $G_3(s)$. In this case, the EBS measures $\omega_{osc} = 0.417$ at the end of Mode 1, producing a $T_1 = 150$ s in Mode 2. Results are presented in Figs. 10 and 11.

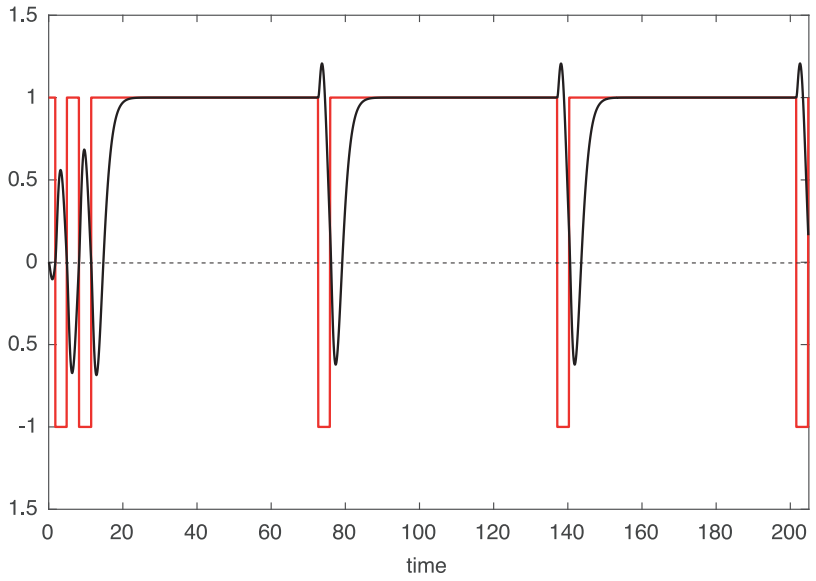

Fig. 6. Simulation of G_2 oscillating at $\omega_{osc} = 0.974$ and $\omega_1 = 0.097$ during Mode 1 and 2, respectively.

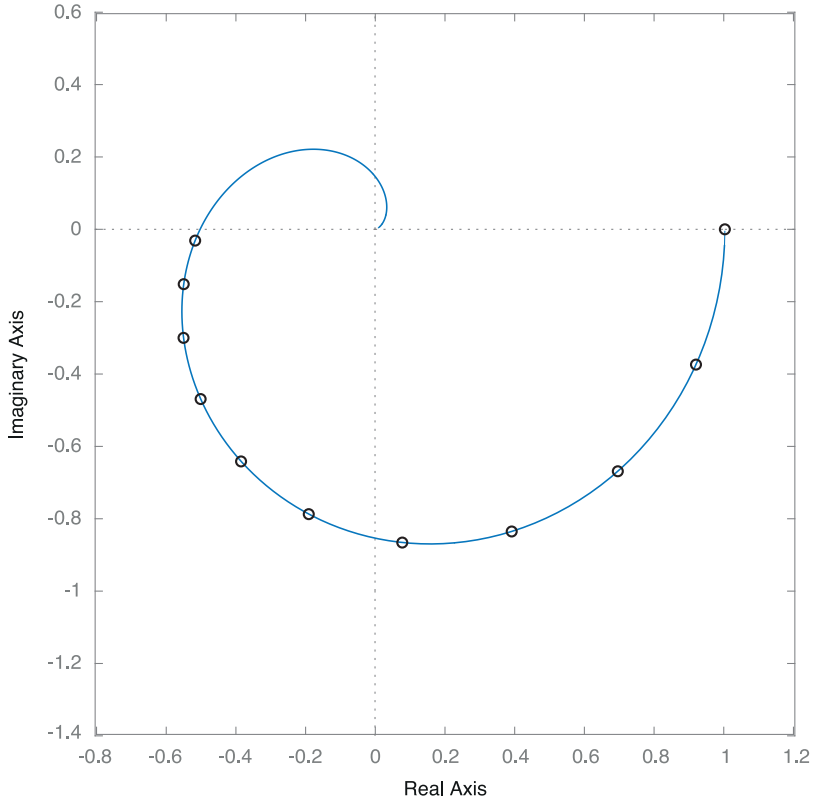

Fig. 7. Nyquist map showing G_2 and the 11 identified points.

In both cases, the results can be considered good and alike to the ones presented in [19,20]. The frequency spectrum is completely discovered between 0 and ω_{osc} for the two processes. The main advantages when compared to these two methods are that the event-based approach can obtain the steady state because it is not based on a symmetric relay and that it produces better results at low frequencies in presence of noise (Section 5 shows the outcomes with more detail).

4.4. Example 4: Influence of ρ in the identification process

A study of the influence of ρ is presented using the four processes of the previous examples. The setup of the experiments is the same that in the previous examples, but different values of ρ are used to study their impact in the quality of the results. To measure the influence of ρ in the identification process, the

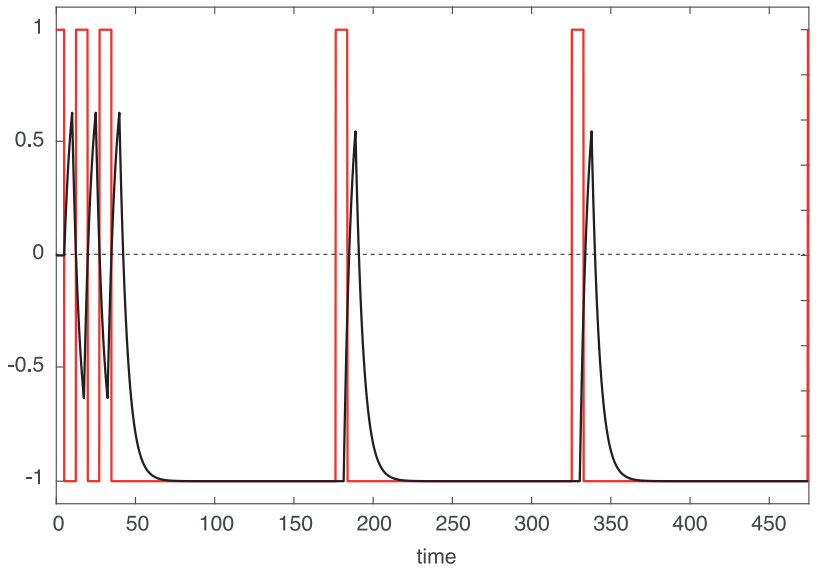

Fig. 8. Simulation of G_3 oscillating at $\omega_{osc} = 0.421$ at $w_1 = 0.042$ during Mode 1 and 2, respectively.

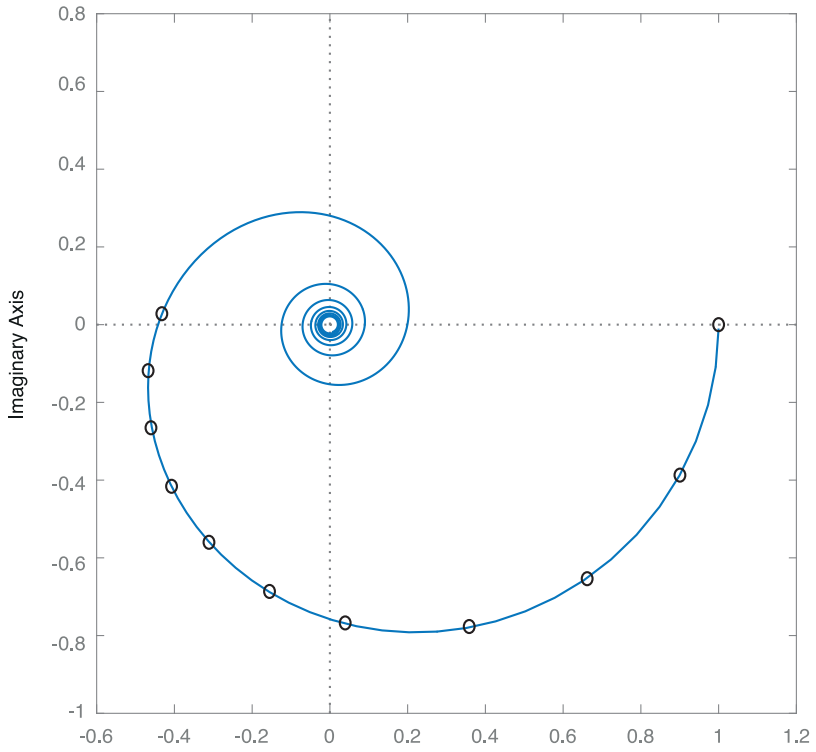

Fig. 9. Nyquist map showing G_3 and the 11 identified points.

following error criterion was calculated for each simulation:

$$Err_N[\%] = 100 \cdot \sum_{k=0}^{N} \frac{|G(jk\omega_1) - \hat{G}(jk\omega_1)|}{|G(jk\omega_1)|} \tag{18}$$

Table 1 presents the results of the experiments. For $N = 10$, the set of ρ to avoid according to Eq. (11) includes 33 values. For the sake of simplicity, Table 1 only presents the results with values of ρ from 0.7 to 0.99 where the ones in bold are the invalid values in the range (0.7, 0.99) according to Eq. (11). The j and i numbers that produce the invalid ρ values are presented to the right, between brackets. The five valid ρ values in the interval (0.7,0.99) have been selected to uniformize the distribution of such values within this interval.

Observing the error criterion, all valid ρ values generate very good results, but some of the invalid ones can produce convenient results too (for example, $\rho = 8/9$). However, there is no guarantee if the value of ρ is randomly selected. It can be stated that the results generated by the procedure are always accurate if $(N-1)/N < \rho < 1$ according with Eq. (11). These experimental results agree with the conclusions in [28].

5. Coping with the noise at the process output

Observing the control scheme of Fig. 1, the EBS is not protected against the presence of noise. The noise in the error signal will produce incorrect triggering of the EBS and the oscillation

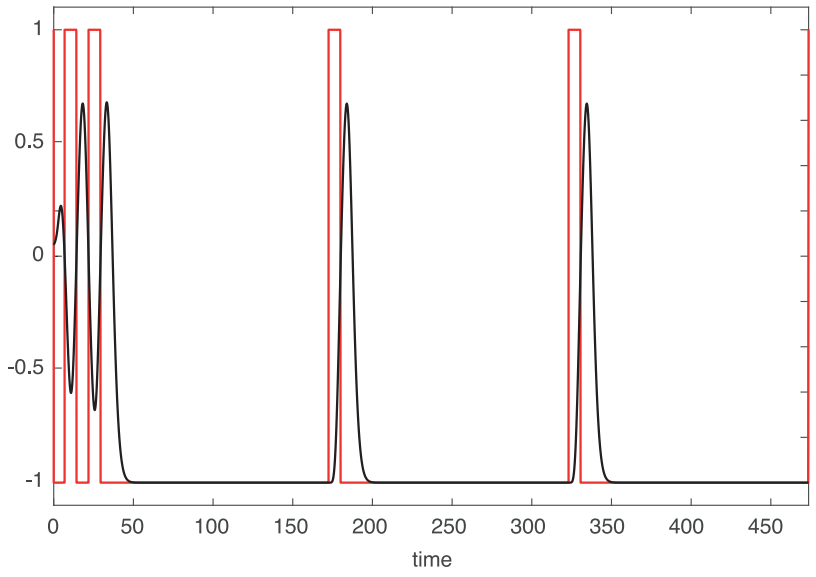

Fig. 10. Simulation of G_4 oscillating at $\omega_{osc} = 0.417$ at $w_1 = 0.041$ during Mode 1 and 2, respectively.

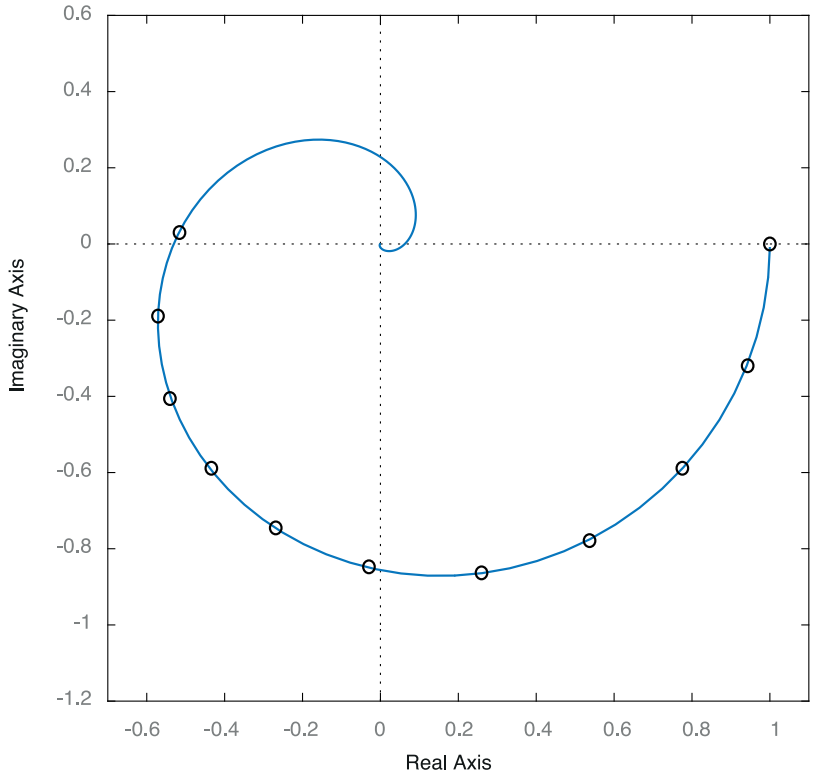

Fig. 11. Nyquist map showing G_4 and the 11 identified points.

frequency ω_{osc} detected during the Mode 1 will be false, spoiling the identification experiment completely. In a classical relay feedback experiment, a common solution is to introduce a hysteresis whose value is slightly greater than the noise amplitude.

The solution proposed is similar and can be appreciated in Fig. 12. The hysteresis can be square because its only purpose is to free $e(t)$ of noise and avoid false triggerings of the EBS. The only condition of the hysteresis is that output and input must have the same sign; the magnitude of the hysteresis output is indifferent as the control action $u(t)$ is sent to the process by the EBS, and it is $\pm D$ (see Eqs. (4) and (6)).

5.1. Example 5: Study of the influence of the noise

To check the robustness of the hysteresis against the noise, the processes of the Examples 1, 2, and 3 were simulated with three different noise levels n_0 whose peak-to-peak amplitude are 0.1, 0.2, and 0.3, and different values of ρ (0.85, 0.95, 0.99). The noise was introduced to the process output and the same seed was used by the noise block in all the simulations. The square hysteresis band was fixed to $1.5n_0$ to protect the EBS, while the rest of parameters of the simulations are the same as in

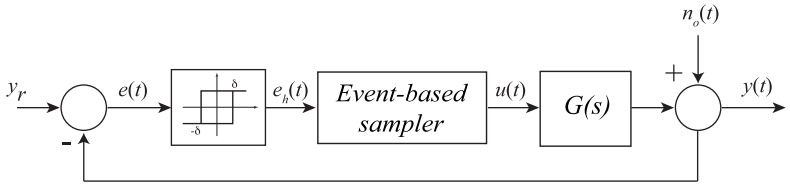

Fig. 12. Event-based feedback control loop to avoid the noise influence.

Table 2
Relative errors of the estimated points for $G_1(s)$.

Err_N [%]	$n_0 = 0.1, \delta = 0.075$	$n_0 = 0.2, \delta = 0.15$	$n_0 = 0.3, \delta = 0.225$
$\rho = 0.85$	1.390	2.310	2.436
$\rho = 0.95$	0.810	1.380	1.650
$\rho = 0.99$	3.157	5.797	6.786
	$\omega_{osc} = 1.157$	$\omega_{osc} = 1.043$	$\omega_{osc} = 0.937$

Table 3
Relative errors of the estimated points for $G_2(s)$.

Err_N [%]	$n_0 = 0.1, \delta = 0.075$	$n_0 = 0.2, \delta = 0.15$	$n_0 = 0.3, \delta = 0.225$
$\rho = 0.85$	0.169	0.338	0.638
$\rho = 0.95$	0.138	0.221	0.348
$\rho = 0.99$	0.432	1.012	1.460
	$\omega_{osc} = 0.946$	$\omega_{osc} = 0.926$	$\omega_{osc} = 0.902$

Table 4
Relative errors of the estimated points for $G_3(s)$.

Err_N [%]	$n_0 = 0.1, \delta = 0.075$	$n_0 = 0.2, \delta = 0.15$	$n_0 = 0.3, \delta = 0.225$
$\rho = 0.85$	0.197	0.384	0.500
$\rho = 0.95$	0.196	0.238	0.271
$\rho = 0.99$	0.504	0.824	1.131
	$\omega_{osc} = 0.411$	$\omega_{osc} = 0.402$	$\omega_{osc} = 0.392$

Table 5
Relative errors of the estimated points for $G_4(s)$.

Err_N [%]	$n_0 = 0.1, \delta = 0.075$	$n_0 = 0.2, \delta = 0.15$	$n_0 = 0.3, \delta = 0.225$
$\rho = 0.85$	0.155	0.319	0.421
$\rho = 0.95$	0.114	0.206	0.252
$\rho = 0.99$	0.438	0.734	0.966
	$\omega_{osc} = 0.410$	$\omega_{osc} = 0.405$	$\omega_{osc} = 0.398$

Examples 1, 2, and 3. To measure the influence of the noise in the identification process, the error criterion of Eq. (18) has been applied. The results are presented in Tables 2, 3, 4, and 5.

From the data of the tables, it can be stated that the identification procedure works well with the protection against the noise based in the hysteresis. In general, the error is below or close to 1%, except for the first process (Table 2). In this case, the increase of the relative errors is consequence of the ratio between the control action and the noise amplitudes. In the experiments associated to Table 2, $D = \pm 0.2$ and the peak-to-peak amplitude of the error goes from 0.1 to 0.3; in the other three tables, $D = \pm 1$. In any case, all the results can be considered acceptable.

Comparing our results in presence of noise with the obtained in [19,20], the relative errors are smaller than those in these two works. In both papers, the relative errors are always over 5% and the biggest differences are in the identified points at the lowest frequencies of the spectrum. That could be a consequence of the approach followed in these two papers. They obtain the points corresponding to the frequencies below ω_{osc} by the measured information of $y(t)$ from the start of the experiment until the process enters in the periodic oscillation status. The influence of the noise in that short period of time can have an excessive impact in the results; however, in the event-based approach, the information is extracted from regular cycles of $y(t)$ of T_1 length, and the impact of the noise is attenuated.

It must be noticed that the inclusion of the hysteresis produces a phase shifting of the critical point detected during the Mode 1, that is, $\hat{G}(j\omega_{osc})$. In the examples without noise, the oscillation frequency detected during the Mode 1 were 1.32, 0.974, 0.421, and 0.417 for the processes G_1, G_2, G_3, and G_4, respectively; the last row of Tables 2, 3, 4, and 5 show the oscillation frequencies detected during the Mode 1 with the hysteresis.

Also, the higher the noise, the more the frequency detected during the Mode 1 decreases. For example, the difference in ω_{osc} between the free-noise experiment of the Example 1 and the same experiment with $n_0 = 0.1$ is 0.162 that corresponds to a phase difference of $-15°$. If the noise is $n_0 = 0.3$, the difference is 0.383 and the phase difference becomes $-40.04°$. To explain the phase shifting phenomena it is necessary to use the describing function theory. The negative reciprocal of the describing function (DF) of a rectangular hysteresis is

$$\frac{-1}{N(A,\delta)} = \frac{-\pi}{4D}\sqrt{A^2-\delta^2} + \frac{-\pi\delta}{4D}j \tag{19}$$

where $A > \delta$ is the amplitude of $e(t)$ and D is the output. Although the hysteresis in Fig. 12 is square and its output is $\pm\delta$, the true output sent to the process during the Mode 1 is the output of the EBS, that is, $\pm D$. Eq. (19) is represented in the Nyquist map as a straight line parallel to the real axis. By increasing δ, the line is moved down along the imaginary axis of the Nyquist map. As the intersection of $G(s)$ with that line means the existence of an oscillation, the critical point $G(j\omega_{osc})$ where the intersection happens is modified by the hysteresis. From Eq. (19), the theoretically phase margin obtained by applying hysteresis is defined by

$$\phi_m = \tan^{-1}\left(\frac{\delta}{\sqrt{A^2-\delta^2}}\right) \tag{20}$$

where it can be appreciated that an increase of the hysteresis produces an increase of the phase shifting of the critical point $G(j\omega_{osc})$.

The true consequence of the phase shifting produced by the hysteresis is that the spectrum of $G(s)$ in the third quadrant is not completely discovered by the experiment. As indicated before, in the Example 1 with $n_0 = 0.1$ the spectrum is identified until $-165°$ (Fig. 13); and with $n_0 = 0.3$ until $-140°$. This issue can be solved by identifying additional points to cover completely the spectrum in the third quadrant of the Nyquist map. To do that it is necessary to increase the value of k in Eq. (8) in the following way

$$\hat{G}(jk\omega_1) = \frac{\int_0^{\frac{2\pi}{\omega_1}} y(t)e^{-jk\omega_1 t}dt}{\int_0^{\frac{2\pi}{\omega_1}} u(t)e^{-jk\omega_1 t}dt} \tag{21}$$

with $k = 0, 1, \ldots, N+M$ where M are the extra points to identify.

So, in the Experiment 1 with $n_0 = 0.1$, $\rho = 0.95$, $N = 10$, and $M = 2$, we obtain the Nyquist plot presented in Fig. 13. The two extra points added let us completely discover the spectrum of G_1 in the third quadrant.

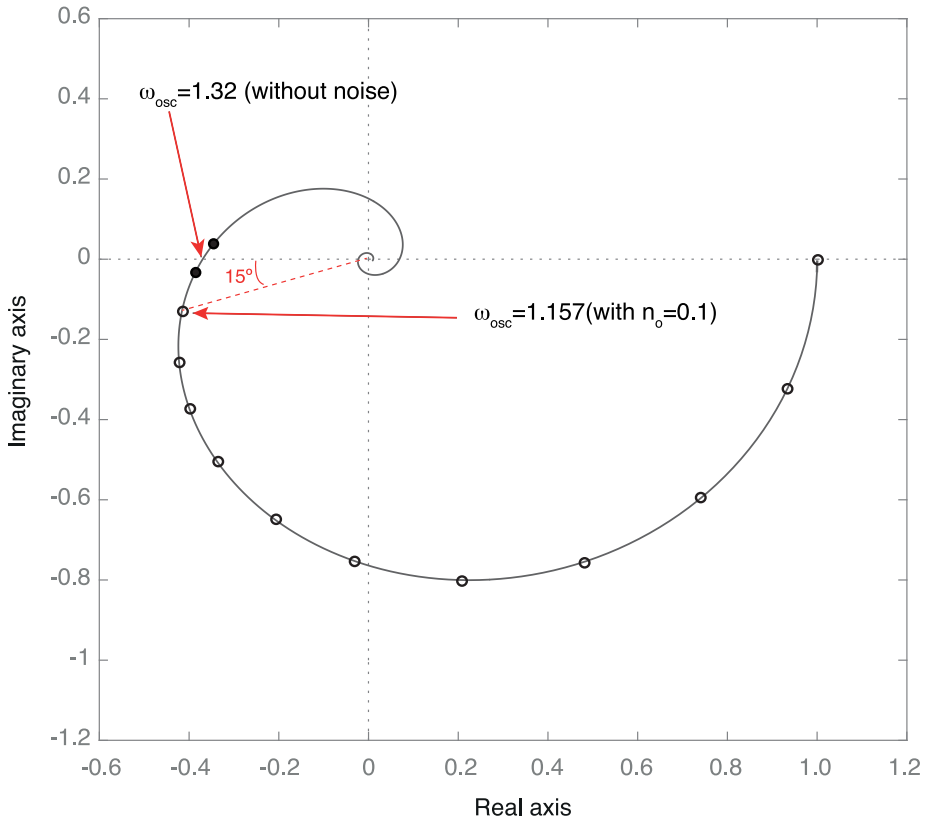

Fig. 13. Nyquist map showing G_1 and the $N = 10$ and additional $M = 2$ identified points (circles and solid dots, respectively).

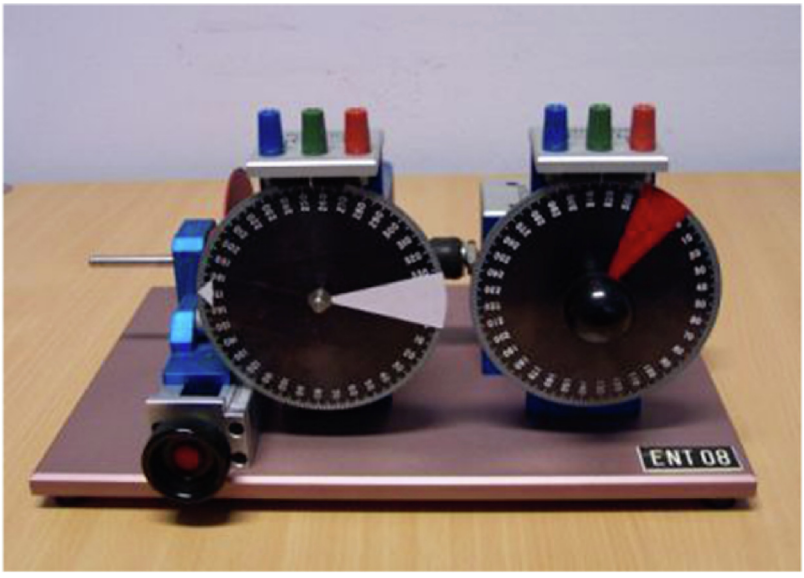

Fig. 14. DC motor of the experimental setup.

6. Real experiments

Real experiments for the identification of the spectrum of a DC motor (Fig. 14) are presented in this section. The experimental setup is a DC motor with a rev counter. The motor moves a load which consists in a steel disc. An adjustable magnetic break applies a viscous friction effect, allowing therefore the modification of the time constant of this first order system, which also includes a dead zone in the area close to where the control signal is null ($u = 0$ V.) The angular position and velocity of the motor are controlled adjusting the input voltage, and the position is measured with a potentiometer connected to the axis of the motor. The output signal presents a low level of noise that allows us adjusting the hysteresis to a minimum.

In the setup of this first experiment, $\rho = 0.9$ and $N = 8$. At the end of Mode 1, the EBS measures $\omega_{osc} = 38$ that produces a real $T_1 = 1.32$ in Mode 2. Figs. 15 and 16 present the identified points and the temporal evolution of the experiments, respectively.

In a second testing scenario, the DC motor has been replaced by another similar, but faulty, to check the procedure in a more

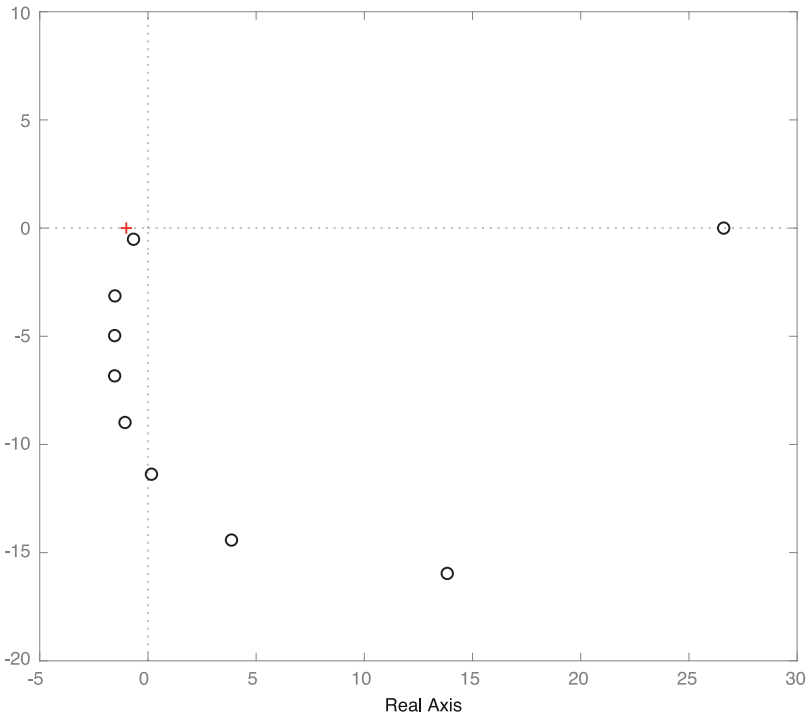

Fig. 15. Nyquist map showing the 10 identified points.

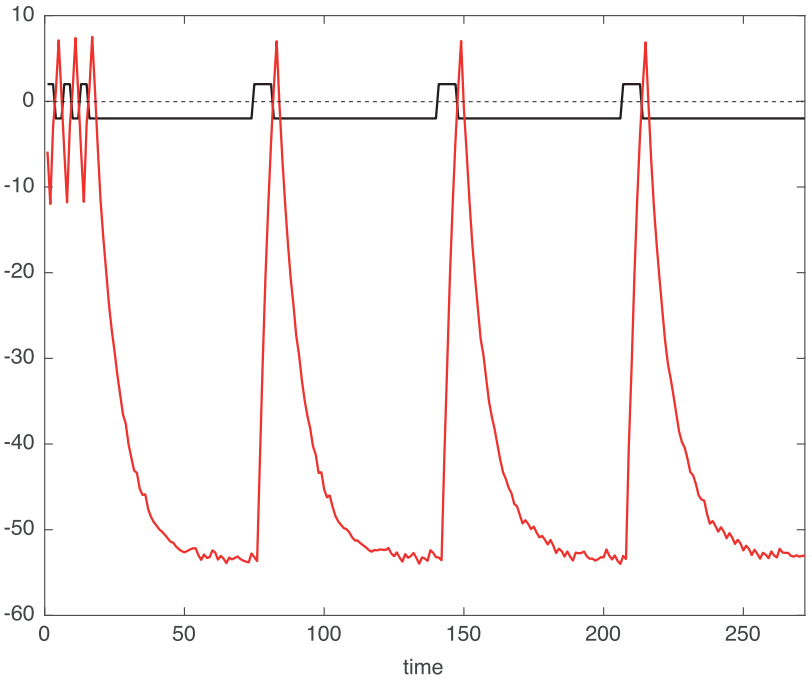

Fig. 16. Signals from the experiment with the DC motor. It can be clearly appreciated the two modes.

realistic scenario: a very noisy output signal that requires to increase the hysteresis to $\pm 4°$; and inner frictions in the gears that produce very irregular cycles of y(t). The experiments have been run with $D = \pm 2$ V, $\rho = 0.95$, and $N = 3$, 5, 10, and 20. Fig. 17 shows the identified spectrums in the four experiments; it can be observed the high impact of the hysteresis that produces that $G(j\omega_{osc})$ is in the fourth quadrant. Table 6 presents the frequencies measured in both modes for the four experiments; the frequency detected during the Mode 1 is similar and in the Mode 2 is function of N.

Table 6
Frequencies measured in the two modes for different values of N.

N	ω_{osc}	ω_1
3	13.560	4.520
5	14.151	2.803
10	13.620	1.362
20	13.628	0.681

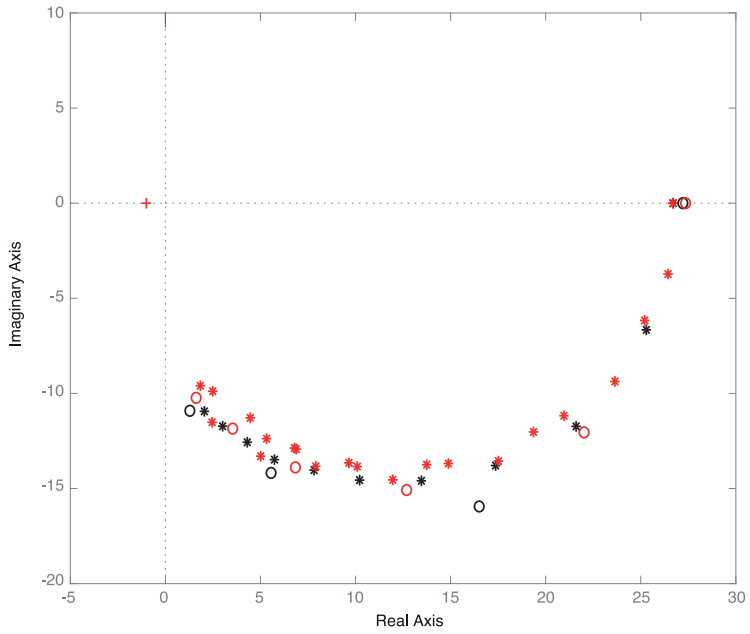

Fig. 17. Nyquist map showing the identified points for N = 3, 5, 10, and 20 (black circles, red circles, black asterisks, and red asterisks, respectively). (For interpretation of the references to colour in this figure legend, the reader is referred to the web version of this article.)

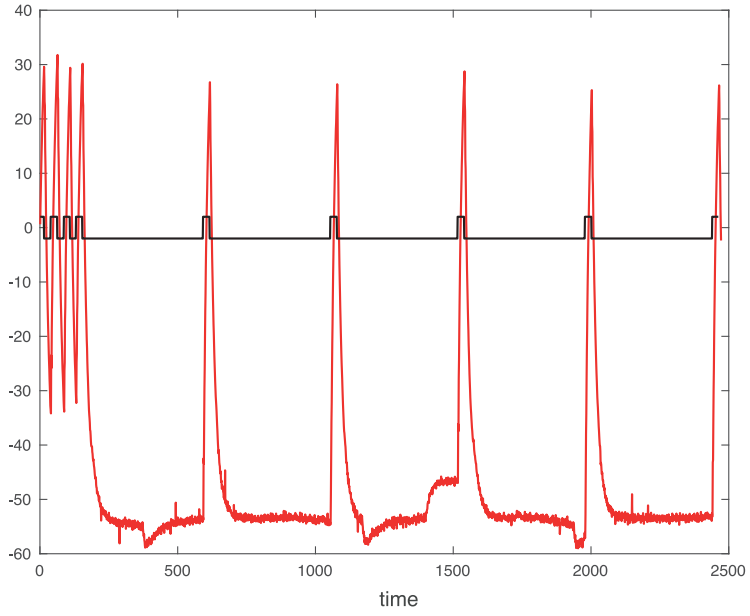

Fig. 18. Signals from an experiment with the faulty DC motor.

Fig. 18 presents the signals of the test for $N = 10$, where the irregular cycles and the high noise are appreciated. The results with the faulty DC motor should be considered valid because its spectrum is clearly depicted, and it matches the spectrum of the first DC motor (Fig. 15).

7. Discussions

The approach seems to work well in all the simulations in the absence of noise. However, if the process output contains noise, it is necessary to protect the EBS from false triggerings that spoil the results of the identification procedure. To solve this, a square hysteresis is placed into the control loop before the EBS. This solution works very well in simulations and real experiments, reducing the impact of the noise in the quality of the results to a minimum. It is important to remark that results are very accurate if $N - 1/N < \rho < 1$ according with Eq. (11). An aleatory selection of ρ could produce good results but the most accurate results will always come from choosing a ρ near 1 (or zero).

In the comparison with other identification procedures with equivalent purposes (Example 3), the accuracy of the current method is similar; however, the duration of the experiments is longer to estimate the same amount of points. The duration of an experimentation can be considerably decreased by a reduction of the number of points to estimate.

Table 7 presents a comparative of the duration of the experiment of Example 1 for different values of N. From the data of the Table 7, it is obvious that the selection of N depends on the data necessary to fulfil the pursued goals. For example, the tuning of a PID controller for a high-order process [30] demands

Table 7
Duration of the experiment with G1(s) for different values of N.

N	Duration	T_1
3	52.40 s.	14.27 s.
5	80.48 s.	23.79 s.
10	150.61 s.	47.59 s.
15	220.87 s.	71.38 s.
20	291.08 s.	95.18 s.

Table 8
Comparative of the experimentation time for different values of N.

N	$G_1(s)$	$G_2(s)$	$G_3(s)$	$G_4(s)$
2	39 s.	50 s.	122 s.	118 s.
3	52 s.	70 s.	167 s.	162 s.
10	150 s.	204 s.	474 s.	473 s.

to know many points of the spectrum for fitting the transfer function template; however, a template of a first order system with time delay can be fitted with only $N = 2$.

Thus, if the procedure is just applied to discover 2 or 3 points (as most of the relay-based identification procedures do), the experimentation time can be reduced considerably: around 75% for N = 2, and 66% for N = 3 (see Table 8).

To sum up the advantages of the described method, it can be mentioned its low mathematical complexity that simplifies its programming, its robustness against the noise than can be obtained by adding a hysteresis, the estimation of $G(0)$ thanks to the asymmetry of $u(t)$, its flexibility to identify many or just a few points below the cross-over frequency, and the possibility of discovering M additional points located at frequencies higher than ω_{osc}. A final advantage is that the logic used in an already existing relay feedback experiment could be maintained by substituting the relay by the EBS block.

8. Conclusions

An event-based approach for discovering the frequency spectrum of stable process in the fourth and third quadrant of the Nyquist map has been presented in the paper. The approach consists in introducing an EBS working in two modes in the control loop to force the oscillation of the system at two different frequencies. During the first mode, the behaviour of the EBS is like a relay and lets us approximate the cross-over frequency ω_{osc}. With this data and the number of points, N, to discover of the frequency spectrum, the second mode of the EBS is programmed and the system is forced to oscillate at a low frequency ω_1.

This identification approach can be considered a step forward in providing a complete event-based autotuning solution. The sampler of, for example, a SSOD-PI controller, can be easily reprogrammed to include the two modes of the identification approach and use the information to tune the controller using some method of the literature (for example, [24,31]).

Declaration of competing interest

The authors declare that they have no known competing financial interests or personal relationships that could have appeared to influence the work reported in this paper.

Acknowledgements

This work was supported in part by the State Research Agency under project PID2020-112658RBI00/10.13039/501100011033.

References

[1] Åström K, Hägglund T. Automatic tuning of simple regulators with specifications on phase and amplitude margins. Automatica 1984;20(5):645—651. http://dx.doi.org/10.1016/0005-1098(84)90014-1.
[2] Liu T, Wang QG, Huang HP. A tutorial review on process identification from step or relay feedback test. J Process Control 2013;23(10):1597–623. http://dx.doi.org/10.1016/j.jprocont.2013.08.003.
[3] Dharmalingam K, Thangavelu T. Parameter estimation using relay feedback. Rev Chem Eng 2018. http://dx.doi.org/10.1515/revce-2017-0099.
[4] Li W, Eskinat E, Luyben W. An improved autotune identification method. Ind Eng Chem Res 1991;30(7):1530–41. http://dx.doi.org/10.1021/ie00055a019.
[5] Tan KK, Lee TH, Wang QG. An enhanced automatic tuning procedure for PI/PID controllers for process control. AIChE J 1996;42:2555–62. http://dx.doi.org/10.1002/aic.690420916.
[6] Scali C, Marchetti G, Semino D. Relay with additional delay for identification and autotuning of completely unknown processes. Ind Eng Chem Res 1999;38(5):1987–97. http://dx.doi.org/10.1021/ie980616l.
[7] Sánchez J, Bencomo SD, Martínez JD. Fitting of generic process models by an asymmetric short relay feedback experiment: The n-shifting method. Appl Sci 2021;11(4):1651. http://dx.doi.org/10.3390/app11041651.
[8] Friman M, Waller KV. A two-channel relay for autotuning. Ind Eng Chem Res 1997;36(7):2662–71. http://dx.doi.org/10.1021/ie970013u.
[9] Wang Y, Shao H. PID autotuner based on gain-and phase-margin specifications. Ind Eng Chem Res 1999;38(8):3007–12. http://dx.doi.org/10.1021/ie9808007.
[10] Sung SW, Lee J, Lee DH, Han JH, Park YS. Two-channel relay feedback method under static disturbances. Ind Eng Chem Res 2006;45(12):4071–4. http://dx.doi.org/10.1021/ie0513393.
[11] Kula K. Online SOPDT model identification method using a relay. Appl Sci 2023;13(1):632. http://dx.doi.org/10.3390/app13010632.
[12] Hang CC, Åström K, Wang QG. Relay feedback auto-tuning of process controllers. a tutorial review. J Process Control 2002;12(1):143–62. http://dx.doi.org/10.1016/S0959-1524(01)00025-7.
[13] Shen SH, Wu JS, Yu CC. Use of biased-relay feedback for system identification. AIChE J 1996;42:1174–80. http://dx.doi.org/10.1002/aic.690420431.
[14] Wang Q, Hang C, Zou B. Low-order modeling from relay feedback. Ind Eng Chem Res 1997;36(2):375–81. http://dx.doi.org/10.1021/ie960412+.
[15] Wang Q, Lee T, Chong L. Relay feedback: analysis, identification and control. Springer Science & Business Media; 2012, http://dx.doi.org/10.1007/978-1-4471-0041-6.
[16] Lee J, Kim JS, Byeon J, Sung SW, Edgar TF. Relay feedback identification for processes under drift and noisy environments. AIChE J 2011;57:1809–16. http://dx.doi.org/10.1002/aic.12394.
[17] Byeon J, Kim J, Sung S, Ryoo W, Lee J. Third quadrant Nyquist point for the relay feedback autotuning of PI controllers. Korean J Chem Eng 2011;28:342–7. http://dx.doi.org/10.1007/s11814-010-0391-4.
[18] Wang Q, Hang C, Bi Q. Process frequency response estimation from relay feedback. Control Eng Pract 1997;5(9):1293–302. http://dx.doi.org/10.1016/S0967-0661(97)84368-7.
[19] Wang Q, Hang C, Bi Q. A technique for frequency response identification from relay feedback. IEEE Trans Control Syst Technol 1999;7(1):122–8. http://dx.doi.org/10.1109/87.736766.
[20] Ma M, Zhu X. A simple auto-tuner in frequency domain. Comput Chem Eng 2006;30(4):581–6. http://dx.doi.org/10.1016/j.compchemeng.2005.09.004.
[21] Cheon Y, Jeon C, Lee J, Sung S. Improved Fourier transform to estimate frequency responses. Korean J Chem Eng 2009;26:925—929. http://dx.doi.org/10.1007/s11814-009-0155-1.
[22] Kim K, Cheon YJ, Lee I-B, Lee J, Sung SW. A frequency response identification method for discrete-time processes with cyclic steady state conditions. Automatica 2014;50(12):3260–7. http://dx.doi.org/10.1016/j.automatica.2014.10.052.
[23] Sánchez J, Guinaldo M, Visioli A, Dormido S. Enhanced event-based identification procedure for process control. Ind Eng Chem Res 2018;57(21):7218–31. http://dx.doi.org/10.1021/acs.iecr.7b05239.
[24] Sánchez J, Guinaldo M, Visioli A, Dormido S. Identification and tuning methods for PI control systems based on symmetric send-on-delta sampling. Int J Control Autom Syst 2019;17:2784–95. http://dx.doi.org/10.1007/s12555-018-0911-2.
[25] Wang P, Gu D, Zhang W. Modified relay feedback identification based on describing function analysis. Ind Eng Chem Res 2007;46(5):1538–46. http://dx.doi.org/10.1021/ie061141y.
[26] Hofreiter M. Shifting method for relay feedback identification. IFAC-PapersOnLine 49(12):1933–8. http://dx.doi.org/10.1016/j.ifacol.2016.07.913.
[27] Berner J, Hägglund T, Åström K. Asymmetric relay autotuning–practical features for industrial use. Control Eng Pract 2016;54:231–45. http://dx.doi.org/10.1016/j.conengprac.2016.05.017.

[28] Miguel-Escrig O, Romero-Pérez JA, Sánchez-Moreno J, Dormido-Bencomo S. Multiple frequency response points identification through single asymmetric relay feedback experiment. Automatica 2023;147:110749. http://dx.doi.org/10.1016/j.automatica.2022.110749.

[29] Wang Q, Fung H, Zhang Y. Robust estimation of process frequency response from relay feedback. ISA Trans 1999;38(1):3–9. http://dx.doi.org/10.1016/s0019-0578(99)00006-3.

[30] Malwatkar GM, Sonawane SH, Waghmare LM. Tuning PID controllers for higher-order oscillatory systems with improved performance. ISA Trans 2009;48(3):347–53. http://dx.doi.org/10.1016/j.isatra.2009.04.005.

[31] Sánchez J, Guinaldo M, Visioli A, Dormido S. Validity of continuous tuning rules in event-based PI controllers using symmetric send-on-delta sampling: An experimental approach. Comput Chem Eng 2020;139:106878. http://dx.doi.org/10.1016/j.compchemeng.2020.106878.